Aurora B dynamics at centromeres create a diffusion-based phosphorylation gradient

Enxiu Wang, Edward R. Ballister, and Michael A. Lampson

Department of Biology, University of Pennsylvania, Philadelphia, PA 19104

Aurora B kinase is essential for successful cell division and regulates spindle assembly and kinetochore–microtubule interactions. The kinase localizes to the inner centromere until anaphase, but many of its substrates have distinct localizations, for example on chromosome arms and at kinetochores. Furthermore, substrate phosphorylation depends on distance from the kinase. How the kinase reaches substrates at a distance and how spatial phosphorylation patterns are determined are unknown. In this paper, we show that a phosphorylation gradient is produced by Aurora B concentration and activation at centromeres and release and diffusion to reach substrates at a distance. Kinase concentration, either at centromeres or at another chromosomal site, is necessary for activity globally. By experimentally manipulating dynamic exchange at centromeres, we demonstrate that the kinase reaches its substrates by diffusion. We also directly observe, using a fluorescence resonance energy transfer–based biosensor, phosphorylation spreading from centromeres after kinase activation. We propose that Aurora B dynamics and diffusion from the inner centromere create spatial information to regulate cell division.

Introduction

Aurora B kinase regulates multiple different processes in cell division, including spindle assembly, kinetochore–microtubule interactions, and cytokinesis. Before anaphase, the kinase is concentrated at the inner centromere as part of the chromosome passenger complex (CPC), which includes the inner centromere protein (INCENP), Survivin, and Borealin. Paradoxically, Aurora B regulates processes at the outer kinetochore and spindle, which are spatially distinct from the inner centromere. Substrates have been identified at the inner centromere (mitotic centromere-associated kinesin), on bulk chromatin (histone H3), at the outer kinetochore (KNL-1/Mis12 complex/Ndc80 complex network), and in the cytoplasm (Op18/stathmin; Hsu et al., 2000; Andrews et al., 2004; Lan et al., 2004; Ohi et al., 2004; Cheeseman et al., 2006; DeLuca et al., 2006; Gadea and Ruderman, 2006; Kelly et al., 2007; Welburn et al., 2010), and an artificial substrate targeted to spindle microtubules is also phosphorylated by Aurora B (Tseng et al., 2010). The differential localization of Aurora B relative to its substrates is important mechanistically, as phosphorylation of outer kinetochore substrates depends on their spatial separation from the kinase, which underlies the regulation of kinetochore–microtubule interactions (Liu et al., 2009). However, it is unclear how Aurora B concentrated at the inner centromere contacts its substrates at distinct sites and how phosphorylation depends on distance from the kinase.

To approach this question, we considered several Aurora B regulatory mechanisms. Clustering of the CPC with anti-INCENP antibodies activates Aurora B in vitro (Kelly et al., 2007), most likely because phosphorylation of the INCENP C terminus in trans activates the kinase (Bishop and Schumacher, 2002; Honda et al., 2003; Sessa et al., 2005). Concentration of Aurora B at centromeres might have a similar effect on kinase activity in vivo. Aurora B and other CPC components also dynamically exchange at the inner centromere (Murata-Hori and Wang, 2002; Beardmore et al., 2004; Ahonen et al., 2009), and Aurora B is inactivated by cytoplasmic phosphatases (Kelly et al., 2007). How spatial regulation of Aurora B activity depends on the combination of local concentration at centromeres, kinase activation, dynamics, and cytoplasmic inactivation is unknown.

E. Wang and E.R. Ballister contributed equally to this paper.

Correspondence to Michael A. Lampson: lampson@sas.upenn.edu

E. Wang's present address is Dept. of Pathology and Laboratory Medicine, School of Medicine, University of Pennsylvania, Philadelphia, PA 19104.

Abbreviations used in this paper: CPC, chromosome passenger complex; INCENP, inner centromere protein; wt, wild type.

The Rockefeller University Press $30.00
J. Cell Biol. Vol. 194 No. 4 539–549
www.jcb.org/cgi/doi/10.1083/jcb.201103044

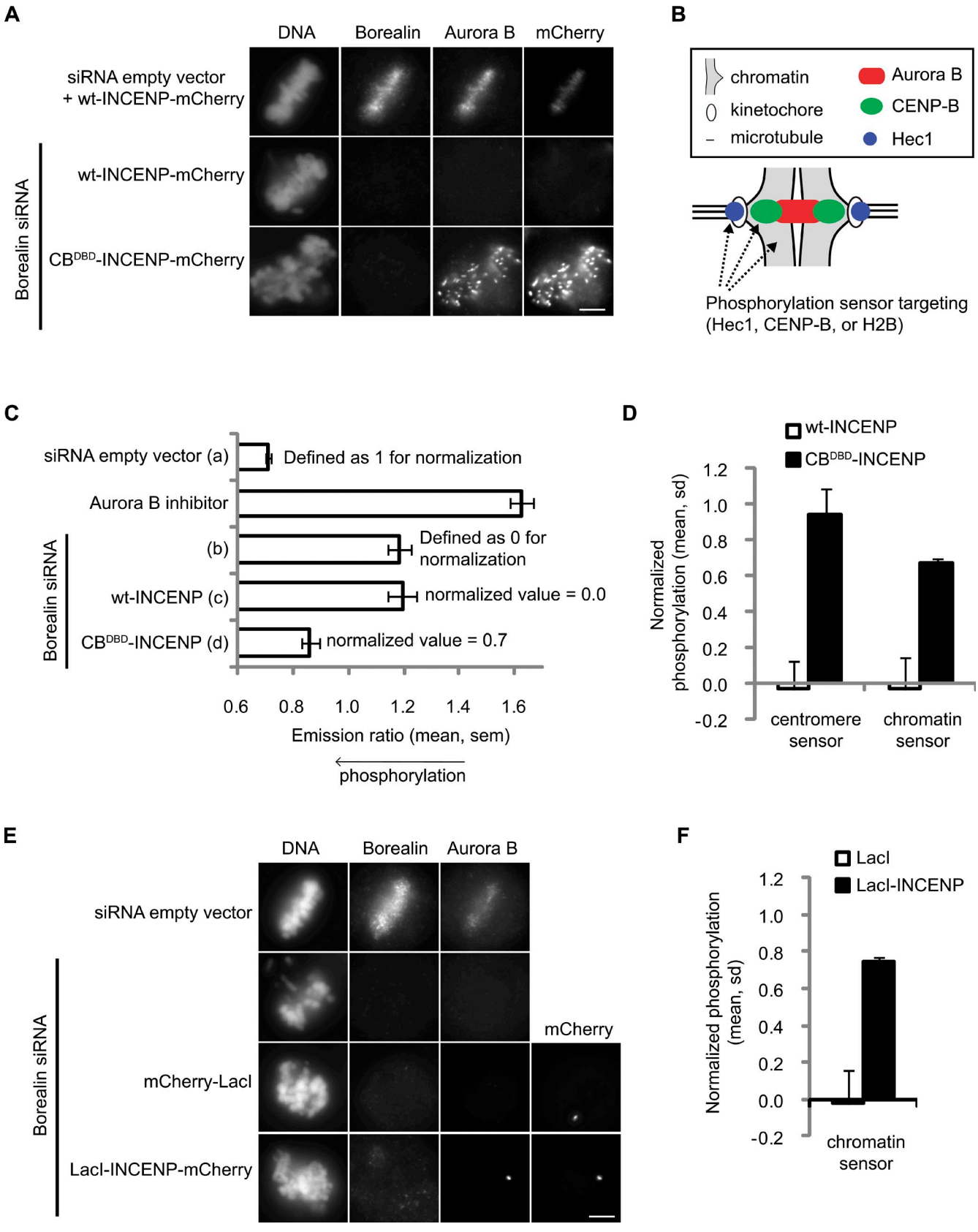

Figure 1. **Local concentration of Aurora B is required for kinase activity.** (A) HeLa cells were transfected with either INCENP-mCherry or CB^{DBD}–INCENP-mCherry with or without Borealin siRNA as indicated and fixed and stained for DNA, Borealin, and Aurora B. (B) A schematic showing targeting of phosphorylation sensors by fusion to Hec1 (kinetochores), CB (centromeres), or histone H2B (bulk chromatin). (C) Cells were transfected as described in A, together with an Aurora B phosphorylation sensor targeted to chromatin, and imaged live. The YFP/CFP emission ratio was analyzed to measure phosphorylation changes and averaged over multiple cells (n = 12 cells for each bar). 2 µM ZM was used to dephosphorylate the sensor, which is

Table I. **Notation for phosphorylation sensors and INCENP fusion proteins targeted to different locations**

Targeting domain	Localization	Phosphorylation sensor	INCENP fusion protein
CB^{DBD}	Centromere	Centromere sensor	CB^{DBD}-INCENP, fast turnover
CB^{FL}	Centromere	NA	CB^{FL}-INCENP, slow turnover
Histone H2B	Chromatin	Chromatin sensor	NA
Hec1	Outer kinetochore	Kinetochore sensor	NA
LacI	*lac* operator array	NA	LacI-INCENP

NA, not applicable.

Results and discussion

Aurora B activity depends on concentration and INCENP phosphorylation

To test whether CPC concentration at centromeres contributes to kinase activation, we designed a strategy to manipulate centromere localization. Borealin depletion by RNAi prevents centromere localization of Aurora B and INCENP (Gassmann et al., 2004; Sampath et al., 2004), but a fusion protein between INCENP and the DNA-binding domain of CENP-B (CB; CB^{DBD}-INCENP; Liu et al., 2009) targets Aurora B to centromeres independent of Borealin (Figs. 1 A and S1 A). Therefore, we compared Borealin-depleted cells expressing either wild type (wt)–INCENP or CB^{DBD}-INCENP, as only CB^{DBD}-INCENP targets to centromeres. To examine Aurora B activity both at centromeres and at a distance from the centromere, we used a fluorescence resonance energy transfer–based biosensor that reports on phosphorylation by Aurora B (Fuller et al., 2008). The sensor is fused either to CB^{DBD} for centromere targeting or to histone H2B for chromatin targeting (Fig. 1 B and Table I). Both centromere- and chromatin-targeted sensors were dephosphorylated in Borealin-depleted cells (Fig. 1, C and D), though the dephosphorylation was incomplete compared with cells treated with the Aurora B inhibitor ZM447439 (ZM). This result is consistent with a previous finding that histone H3 Ser10 phosphorylation is inhibited more completely by ZM than by INCENP depletion (Xu et al., 2009). We also expressed CB^{DBD}-INCENP or wt-INCENP in Borealin-depleted cells to determine the contribution of kinase localization to kinase activity. We normalized each experiment on a phosphorylation scale of 0–1, determined by Borealin-depleted and control cells with wt CPC (Fig. 1 C). Normalized results were used to average multiple experiments and to compare different targeted phosphorylation sensors. Expression of CB^{DBD}-INCENP but not wt-INCENP restored phosphorylation of both centromere- and chromatin-targeted sensors (Fig. 1 D). This finding indicates that concentration of Aurora B at centromeres contributes to kinase activity both locally at centromeres and globally on chromatin.

If kinase concentration leads to activation, we predict that localization to a noncentromere site should also restore activity in Borealin-depleted cells. To test this prediction, we designed a system to target INCENP and Aurora B to a different chromosomal site. A human U2OS cell line with a *lac* operator array integrated into a euchromatic region on chromosome 1 (U2OS-LacO) has been used to target the lac repressor protein (LacI) to the site of the array (Janicki et al., 2004). Expression of a LacI-INCENP fusion protein in these cells together with depletion of Borealin targeted Aurora B to a spot on the chromatin rather than to centromeres (Fig. 1 E). Furthermore, phosphorylation of the chromatin-targeted sensor in Borealin-depleted cells was restored by expression of LacI-INCENP (Fig. 1 F). Together, these results demonstrate that global Aurora B activity in vivo requires kinase concentration either at centromeres or elsewhere in the cell.

To test whether Aurora B activation by concentration at centromeres depends on phosphorylation of the C-terminal Thr-Ser-Ser (TSS) motif of INCENP, we measured the effects of mutating the TSS to Ala-Ala-Ala (AAA) in the context of the CB^{DBD}-INCENP fusion protein. We used targeted phosphorylation sensors to examine phosphorylation at different sites (Fig. 1 B and Table I). CB^{DBD}-$INCENP^{TSS/AAA}$ restored phosphorylation of the centromere-targeted sensor in Borealin-depleted cells, although not to the same level as CB^{DBD}-INCENP (Fig. 2 A). However, CB^{DBD}-$INCENP^{TSS/AAA}$ did not restore phosphorylation of the chromatin-targeted sensor. INCENP can partially activate Aurora B without TSS phosphorylation (Sessa et al., 2005), which suggests that partial kinase activity is sufficient to phosphorylate substrates that localize to the same site as the kinase but not substrates at a distance. As another test of kinase activity, we measured phosphorylation of a sensor targeted to the outer kinetochore (Liu et al., 2010). Expression of CB^{DBD}–INCENP restored phosphorylation of this sensor in Borealin-depleted cells, but expression of CB^{DBD}-$INCENP^{TSS/AAA}$ did not (Fig. 2 A). This result indicates that phosphorylation of substrates at a distance from the kinase, either at the outer kinetochore or on chromosome arms, requires full activation by phosphorylation of the INCENP C terminus.

indicated by an increased emission ratio. The letters to the left of the vertical axis indicate how normalized phosphorylation was calculated: (c − b)/(a − b) for wt-INCENP or (d − b)/(a − b) for CB^{DBD}–INCENP. (D) The experiment described in C was repeated with sensors targeted either to centromeres or to chromatin. Normalized values were calculated for each experiment as in C and averaged over three independent experiments. (E) U2OS-LacO cells were transfected with mCherry-LacI or with LacI-INCENP–mCherry with or without Borealin siRNA as indicated and then were fixed and stained for DNA, Borealin, and Aurora B. (F) Cells were transfected as described in E, together with the chromatin-targeted Aurora B phosphorylation sensor, and imaged live. The normalized YFP/CFP emission ratio was averaged over three independent experiments. Bars, 5 µm.

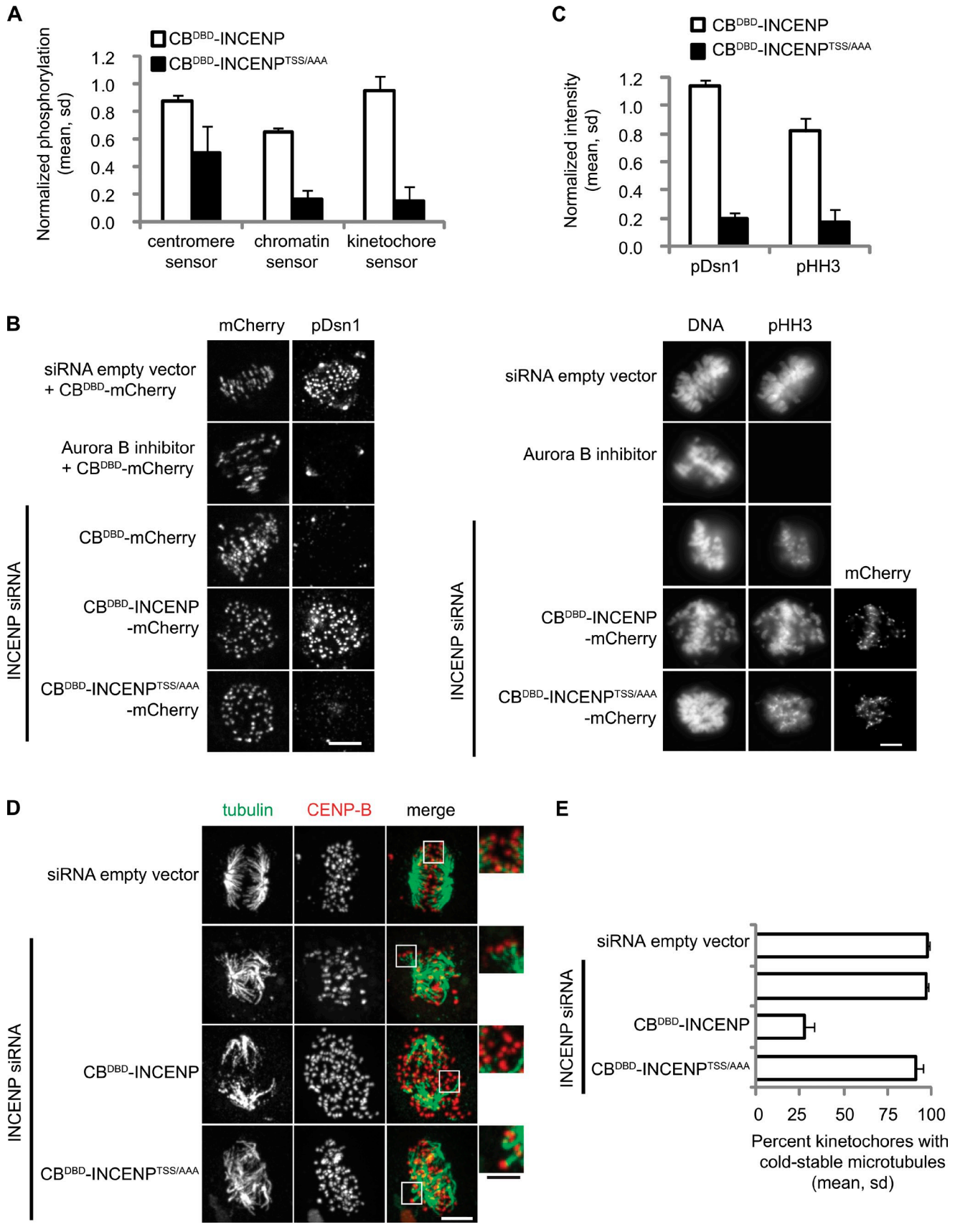

Figure 2. **Aurora B activity at a distance depends on phosphorylation of INCENP.** (A) HeLa cells were transfected with either CB^{DBD}-INCENP–mCherry or CB^{DBD}-$INCENP^{TSS/AAA}$–mCherry, together with an Aurora B phosphorylation sensor targeted either to centromeres, chromatin, or kinetochores. Cells were also treated with or without Borealin siRNA and imaged live. The normalized YFP/CFP emission ratio or YFP/TFP for the kinetochore-targeted sensor was

To determine the importance of INCENP phosphorylation for kinase activity toward endogenous substrates, we used phospho-specific antibodies toward Aurora B sites on chromatin (histone H3 Ser10) and at the outer kinetochore (Dsn1 Ser100; Hsu et al., 2000; Welburn et al., 2010). Both substrates are dephosphorylated in INCENP-depleted cells, though to different degrees. H3 Ser10 was still partially phosphorylated, consistent with a previous study (Xu et al., 2009), but the absence of detectable Dsn1 Ser100 phosphorylation may reflect higher phosphatase activity at kinetochores as a result of PP1 localization (Trinkle-Mulcahy et al., 2003; Liu et al., 2010). Phosphorylation of both H3 Ser10 and Dsn1 Ser100 was restored in INCENP-depleted cells expressing siRNA-resistant CB^{DBD}-INCENP but not in cells expressing CB^{DBD}-$INCENP^{TSS/AAA}$ (Fig. 2, B and C).

Because phosphorylation of outer kinetochore substrates destabilizes kinetochore microtubules, we analyzed cold-stable microtubules as a functional assay for kinetochore phosphorylation differences. In INCENP-depleted cells, attachments are destabilized by CB^{DBD}-INCENP but not by CB^{DBD}-$INCENP^{TSS/AAA}$ (Fig. 2, D and E), which is consistent with the analysis of kinetochore substrate phosphorylation (Fig. 2, A–C). We also found that CB^{DBD}-INCENP and CB^{DBD}-$INCENP^{TSS/AAA}$ recruit Aurora B to centromeres equally well (Fig. S1, C–E). These findings demonstrate that INCENP phosphorylation is required for kinase activity toward substrates at sites distinct from Aurora B itself.

Aurora B activity toward substrates at a distance depends on dynamics at centromeres

Our results indicate that phosphorylation of substrates at a distance requires Aurora B concentration and activation at centromeres, suggesting that the kinase reaches substrates at other sites by release and diffusion. To test this model, we designed a strategy to manipulate INCENP dynamics at centromeres in vivo. CB^{DBD} exchanges more rapidly than full-length CB (CB^{FL}) at mitotic centromeres (Hemmerich et al., 2008), which allowed us to design INCENP fusion proteins with different turnover rates (Table I). Indeed, FRAP measurements show that CB^{FL}-INCENP exchanges very slowly at centromeres, whereas CB^{DBD}-INCENP recovers to ∼40% of prebleach levels within ∼2 min (Fig. 3, A and B). We constructed both CB-INCENP fusion proteins to be siRNA resistant and expressed them in cells depleted of endogenous INCENP (Fig. S1 B). Both CB^{DBD}-INCENP and CB^{FL}-INCENP targeted Aurora B to centromeres and restored phosphorylation of the centromere-targeted sensor in INCENP-depleted cells (Fig. 3, C and D). This result is expected because the kinase should reach these substrates without diffusion. However, CB^{DBD}–INCENP restored phosphorylation of the chromatin-targeted sensor more effectively than CB^{FL}–INCENP (Fig. 3 D).

We also examined spatial phosphorylation patterns using the chromatin-targeted phosphorylation sensor. To facilitate our analysis, we treated cells with monastrol to create monopolar spindles in which chromosomes are arranged radially around the centrosomes with centromeres oriented toward the center (Mayer et al., 1999). Replacement of endogenous INCENP with CB^{FL}-INCENP generated phosphorylation locally at centromeres, which rapidly decreased with distance from the centromeres (Fig. 3, E and F). In contrast, replacement with CB^{DBD}-INCENP generated phosphorylation all over the chromatin. Together, these results indicate that phosphorylation of substrates at a distance depends on release of INCENP from the centromere, which suggests that the kinase reaches these substrates by diffusion.

In addition to its activation at centromeres, Aurora B activity is suppressed by cytoplasmic phosphatases (Kelly et al., 2007), which suggests a model in which local activation, diffusion, and global inactivation would create a gradient of kinase activity centered at the centromere. We did not observe a phosphorylation gradient on chromosome arms in cells expressing endogenous CPC, which suggests that kinase activity at a distance from the centromere might dominate over phosphatase activity, so that chromatin substrates are uniformly phosphorylated. Partial inhibition of Aurora B might decrease kinase activity to the point at which it is balanced by phosphatase activity on chromosome arms. Therefore, we analyzed phosphorylation of the chromatin-targeted sensor with different concentrations of ZM. At 0.3 µM ZM, the sensor is partially dephosphorylated (Fig. 4 A), and we observed a clear gradient of phosphorylation centered at the centromere in monopolar spindles (Fig. 4, B and C). At 0.1 or 0.5 µM ZM, the sensor is predominantly phosphorylated or dephosphorylated, respectively, and spatial patterns are less pronounced. These findings indicate that there is a gradient of kinase activity centered at the centromere, but differences in phosphorylation are usually not observed because phosphatase activity on chromosome arms is not high enough to oppose the kinase.

We also analyzed spatial phosphorylation patterns in U2OS-LacO cells depleted of endogenous INCENP and expressing LacI-INCENP. In these cells, the chromatin-targeted sensor is uniformly phosphorylated in the absence of kinase inhibitor or uniformly dephosphorylated with 10 µM ZM. At intermediate concentrations of 0.5 or 2 µM ZM, we observed a gradient of phosphorylation around the site at which LacI-INCENP localizes (Fig. 4, D and E). The relatively high levels of LacI-INCENP at the LacO site (Fig. S2 B) may explain why phosphorylation persists at 2 µM ZM, which is sufficient for complete dephosphorylation in cells expressing only endogenous INCENP (Fig. 4 A). To test whether kinase activity at 2 µM ZM is associated with phosphorylation of LacI-INCENP at the C-terminal TSS motif, we generated a phospho-specific antibody against this motif (Salimian et al., 2011). With 2 µM

calculated as described in Fig. 1 C and averaged over three independent experiments. (B and C) Cells were transfected with the indicated constructs with or without INCENP siRNA as indicated and then were fixed and stained for phospho-Dsn1 (pDsn1) Ser100 or phospho-H3 (pHH3) Ser10. Representative images are shown (B), and normalized phospho-Dsn1 or phospho-H3 staining was quantified and averaged over three independent experiments (C). (D and E) Cells transfected as described in B and C were fixed and analyzed for cold-stable microtubules. (D) Images are maximum intensity projections of confocal stacks; the insets are optical sections showing individual kinetochores on the right. (E) The percentage of kinetochores with cold-stable microtubules from multiple cells was averaged over three independent experiments. Bars: (B and D) 5 µm; (D, insets) 2.5 µm.

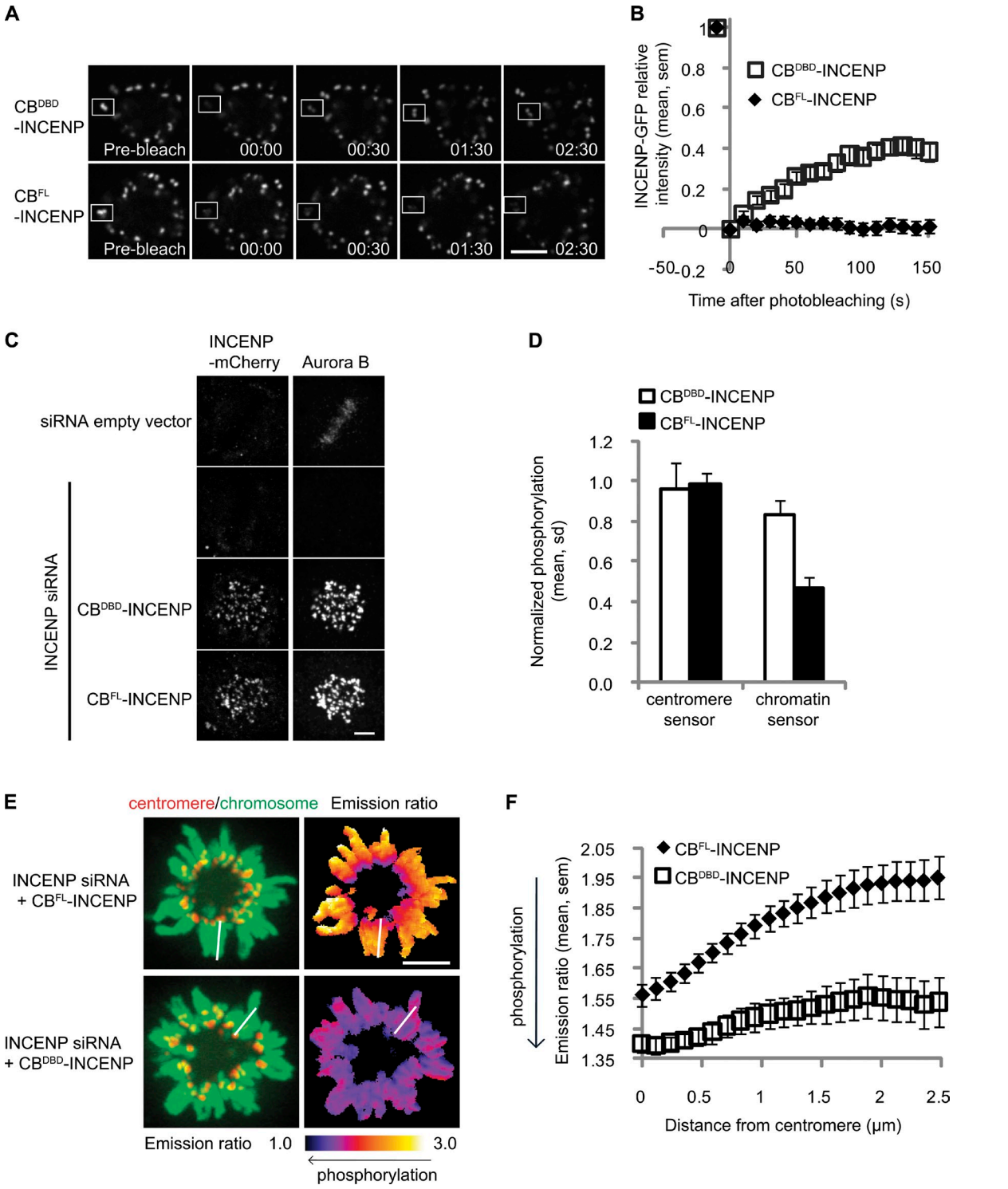

Figure 3. **Aurora B activity at a distance depends on INCENP dynamics at centromeres.** (A and B) Cells were transfected with either CB^{DBD}-INCENP–GFP or CB^{FL}-INCENP–GFP and treated with monastrol to induce monopolar spindles, which facilitates tracking of individual centromeres (indicated by white boxes). Images (A) were acquired before and after bleaching a single pair of centromeres (at time = 0) using a 405-nm laser, and fluorescence intensity was measured at each time point and averaged over multiple cells (each point represents $n \geq 8$ cells; B). (C) Cells were transfected with either CB^{DBD}-INCENP–mCherry or CB^{FL}-INCENP–mCherry with or without INCENP siRNA as indicated and fixed and stained for Aurora B. (D) Cells were transfected as described in C, together with an Aurora B phosphorylation sensor targeted either to centromeres or to chromatin, and imaged live. The normalized YFP/CFP emission ratio was calculated as described in Fig. 1 C and averaged over three independent experiments. (E and F) Cells were transfected with either CB^{DBD}-INCENP–mCherry or CB^{FL}-INCENP–mCherry, together with INCENP siRNA and the chromatin-targeted Aurora B phosphorylation sensor. Cells were treated with monastrol to induce monopolar spindles with centromeres oriented toward the middle and imaged live. (E) The left panels show centromeres (mCherry) and chromosomes (YFP emission), and the right panels show the YFP/CFP emission ratio, color coded as indicated by the color scale. Spatial phosphorylation patterns were analyzed along lines drawn manually extending outward from mCherry-labeled centromeres (white lines). (F) The emission ratio was averaged over multiple line scans (each line represents $n \geq 5$ cells, five centromeres per cell).

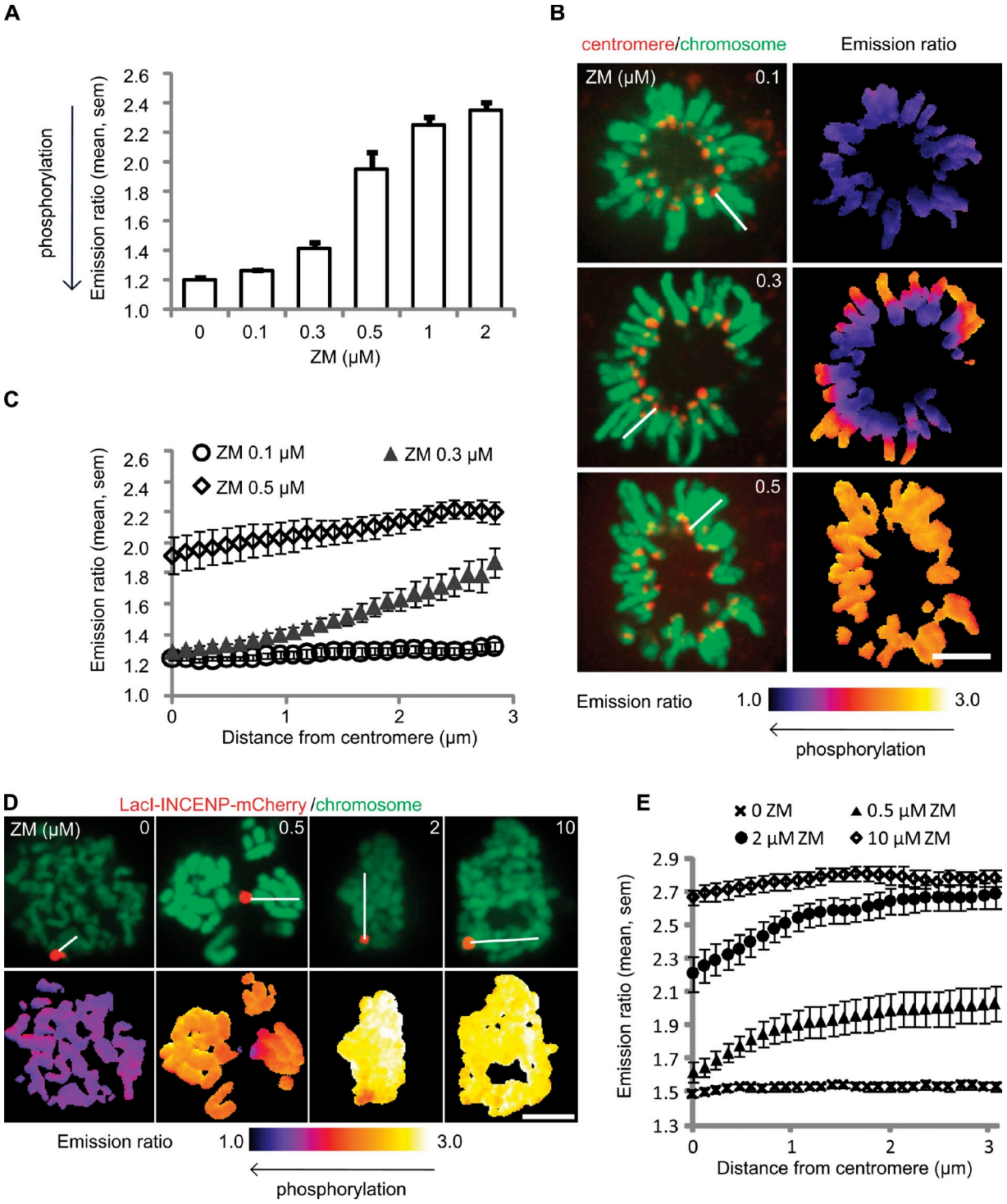

Figure 4. **Partial Aurora B inhibition reveals a spatial phosphorylation gradient.** (A–C) HeLa cells were transfected with the chromatin-targeted Aurora B phosphorylation sensor together with CB-mCherry to label centromeres and then were treated for 1 h with monastrol to orient centromeres toward the middle, MG132 to prevent mitotic exit, and ZM at the indicated concentrations. (A) Cells were imaged live, and the YFP/CFP emission ratio was averaged over multiple cells ($n \geq 6$ for each concentration) to determine concentrations in which phosphorylation is most sensitive to local kinase activity. (B) Images show centromeres and chromosomes and the color-coded YFP/CFP emission ratio. (C) Spatial phosphorylation patterns were analyzed along lines extending out from centromeres (B, white lines). Each curve represents $n \geq 6$ cells, at least four centromeres per cell. (D and E) U2OS-LacO cells were transfected with the chromatin-targeted Aurora B phosphorylation sensor, INCENP siRNA vector, and siRNA-resistant LacI-INCENP–mCherry. Cells were treated for 1 h with nocodazole and ZM at the indicated concentrations and imaged live. (D) Images show LacI-INCENP and chromosomes and the color-coded YFP/CFP emission ratio. (E) Phosphorylation was analyzed along lines extending from the LacI spot (D, white lines). Each curve represents $n \geq 8$ cells, three line scans per cell. Bars, 5 μm.

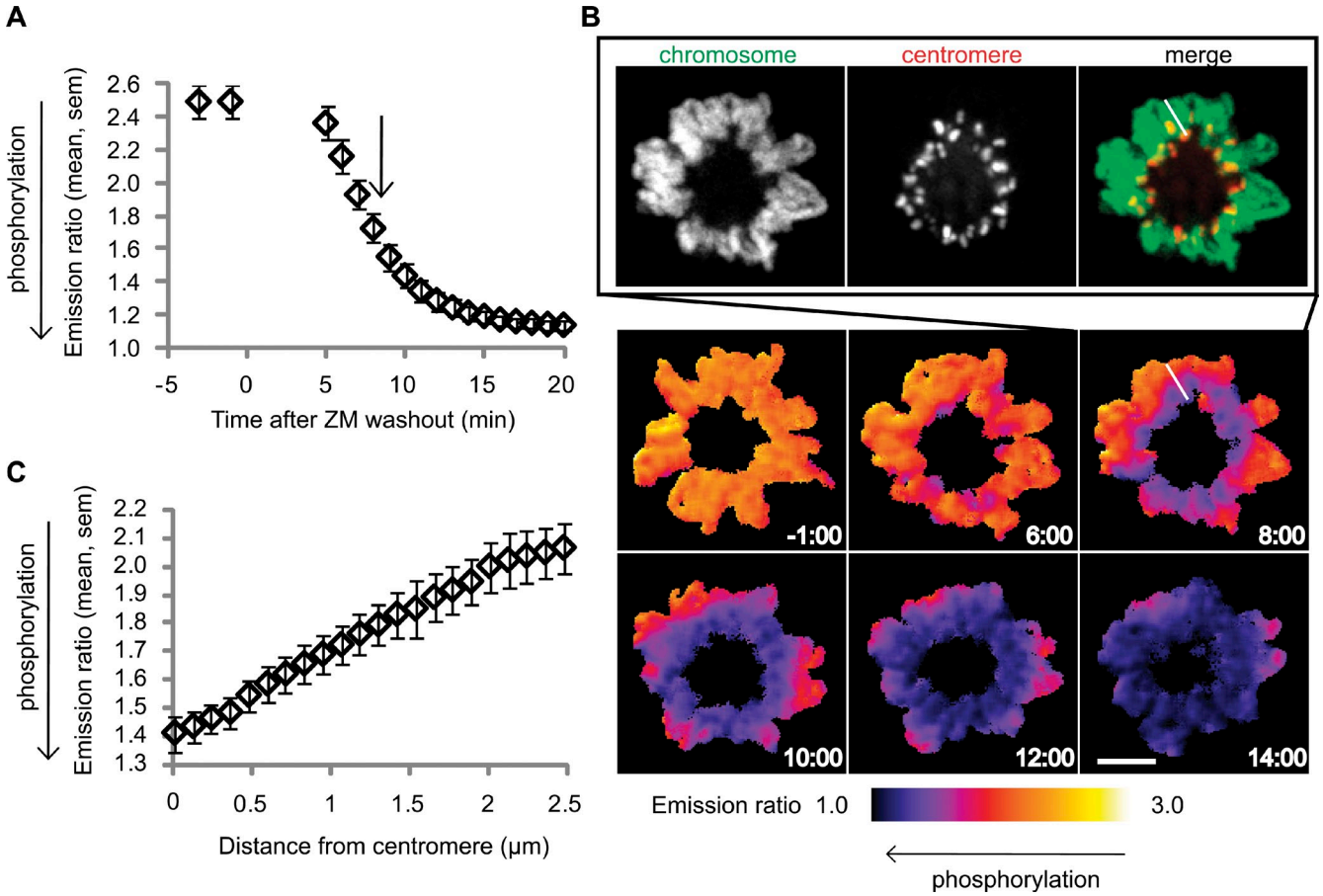

Figure 5. **Real-time observation of phosphorylation spreading from centromeres.** (A–C) Cells were transfected with the chromatin-targeted Aurora B phosphorylation sensor together with CB-mCherry to label centromeres and then were treated with monastrol, MG132, and ZM. Cells were imaged live during activation of Aurora B by ZM washout. (A) The YFP/CFP emission ratio was averaged over multiple cells (n = 11) to determine the kinetics of phosphorylation during ZM washout. The arrow indicates the time point analyzed in C. (B, top) Centromeres (CB-mCherry) and chromosomes (YFP emission) for a single time point. (bottom) Color-coded YFP/CFP emission ratio at different time points. The timestamp (minutes and seconds) is relative to ZM washout at t = 0. Bar, 5 µm. (C) The spatial phosphorylation gradient was analyzed by averaging the emission ratio over lines extending outward from mCherry-labeled centromeres (B, white lines) at t = 8 min (n = 11 cells, four centromeres per cell).

ZM, INCENP is dephosphorylated at centromeres in cells expressing only endogenous INCENP but is highly phosphorylated in U2OS-LacO cells expressing LacI-INCENP (Fig. S2 C). These results suggest that concentration at the LacO site leads to increased INCENP phosphorylation and therefore higher kinase activity, though differences in local phosphatase activity may also contribute.

As another approach to test whether a phosphorylation gradient is generated by Aurora B activation and release from centromeres, we analyzed phosphorylation dynamics during kinase activation. We treated cells with monastrol to create monopolar spindles and with ZM to inhibit Aurora kinase activity, so that the chromatin-targeted phosphorylation sensor starts in the dephosphorylated state. After washing out the inhibitor, we directly observed phosphorylation dynamics during kinase activation (Lampson et al., 2004). Phosphorylation gradually increased after inhibitor washout (Fig. 5 A), with a clear spatial gradient as phosphorylation started at the centromeres and spread over the chromosome arms (Fig. 5 [B and C] and Video 1). The timing of these changes likely reflects a combination of inhibitor washout, kinase turnover and diffusion, and substrate phosphorylation. We also analyzed H3 Ser10 phosphorylation in fixed cells at various times after ZM washout and observed a similar pattern, with phosphorylation beginning at centromeres and gradually spreading over the chromosome arms (Fig. S3). These results demonstrate that the centromere is the source of active kinase, which produces a gradient of kinase activity.

Conclusions

Our results support a model in which Aurora B is locally activated at centromeres by concentration and phosphorylation of the INCENP C terminus followed by release and diffusion of active kinase to reach substrates at a distance. In combination with cytoplasmic phosphatase activity, these dynamics create a phosphorylation gradient centered at the centromere. Many Aurora B substrates do not freely diffuse, for example because they localize to chromosomes, so spatial phosphorylation patterns would be preserved. The model is supported by our experimental manipulations of kinase targeting, INCENP phosphorylation, and INCENP dynamics at the centromere, combined with observations in live cells using targeted biosensors and in fixed cells using phospho-specific antibodies. In *Xenopus*

laevis egg extracts, spindle assembly depends on Aurora B activation through enrichment on chromosomes and likely involves phosphorylation of substrates at a distance on spindle microtubules through a similar diffusion-based mechanism (Kelly et al., 2007; Maresca et al., 2009). Surprisingly, in HeLa cells, Aurora B substrates at centromeres (CENP-A Ser7) and on chromatin (H3 Ser10) are still phosphorylated after depletion of the mitotic kinase Haspin, which inhibits Aurora B localization to centromeres (Wang et al., 2010). However, concentration of Aurora B in other chromosomal regions in these cells (Yamagishi et al., 2010) may be sufficient for kinase activity, similar to what we observed for concentration by LacI-INCENP (Fig. 1, E and F).

Our findings explain how Aurora B phosphorylates substrates at micrometer scale distances from centromeres, such as on chromatin and on spindle microtubules. At kinetochores, however, phosphorylation of outer kinetochore substrates depends on their distance from the inner centromere on submicrometer scales (Liu et al., 2009). We propose that phosphorylation of these substrates depends on their position in a diffusion-based gradient of kinase activity centered at the inner centromere. An alternative model is that outer kinetochore substrates may also be phosphorylated, while the CPC remains bound to the inner centromere (Santaguida and Musacchio, 2009; Maresca and Salmon, 2010), and it remains unclear to what extent Aurora B can phosphorylate kinetochore substrates without diffusion. The phosphorylation gradient that we observed extends over micrometer distances from centromeres on the chromosome arms, similar to a gradient previously observed in anaphase (Fuller et al., 2008), which raises the question of how phosphorylation of kinetochore substrates is regulated on submicrometer distance scales. Localized phosphatase activities may provide an answer. Outer kinetochore substrates are dephosphorylated at metaphase (Liu et al., 2009; Welburn et al., 2010), whereas chromatin substrates remain fully phosphorylated (Hendzel et al., 1997), which indicates that phosphatase activity is higher at kinetochores than on chromatin, consistent with PP1 localization to kinetochores (Trinkle-Mulcahy et al., 2003). These observations suggest that local phosphatase activity may shape a phosphorylation gradient at kinetochores to generate spatial patterns on submicrometer distance scales. Several mechanisms regulate PP1 and PP2A localization at centromeres and kinetochores (Kitajima et al., 2006; Riedel et al., 2006; Tang et al., 2006; Kim et al., 2010; Liu et al., 2010; Posch et al., 2010), and these phosphatases could locally sharpen a phosphorylation gradient by both inactivating Aurora B and directly dephosphorylating substrates. Our findings provide a foundation for understanding how the combination of kinase and phosphatase activities generates a spatial phosphorylation gradient at kinetochores.

Materials and methods

Cell culture and transfection

HeLa and U2OS cells were cultured in growth medium (DME with 10% FBS and penicillin-streptomycin) at 37°C in a humidified atmosphere with 5% CO_2. 100 µg/ml hygromycin B was added to growth medium for the U2OS-LacO cell line (a gift from S.M. Janicki, The Wistar Institute, Philadelphia, PA). Cells were transfected with plasmid DNA using Fugene (Roche) for HeLa cells or Effectene (QIAGEN) for U2OS cells, following the manufacturer's instructions. HeLa cells were used for all experiments, except for the LacI-INCENP experiments, in which we used the U2OS-LacO cell line.

Plasmids

CB^{DBD}-INCENP–mCherry encodes the centromeric CB^{DBD} (aa 1–158), truncated INCENP (aa 47–920), and C-terminal fusion mCherry in vector pcDNA3.1(+). CB^{FL}-INCENP–mCherry and LacI-INCENP–mCherry were generated by replacing CB^{DBD} with either CB^{FL} or with LacI. We swapped GFP for mCherry to create the CB^{DBD}–INCENP-GFP and CB^{DBD}–INCENP-GFP constructs used for FRAP experiments. The $INCENP^{TSS/AAA}$ mutant was created by PCR.

The design of the Aurora B phosphorylation sensors is based on a protein kinase C sensor (Violin et al., 2003), a CFP/YFP (or TFP/YFP) fluorescence resonance energy transfer pair with a substrate peptide and an FHA2 phospho-Thr–binding domain in between. An N-terminal targeting domain localizes the sensor to centromeres (CB fusion), chromatin (H2B fusion), or kinetochores (Hec1 N-terminal fusion) as previously described (Fuller et al., 2008; Liu et al., 2009; Welburn et al., 2010). As with other phosphorylation sensors following this design, a decrease in the YFP/CFP emission ratio indicates increased phosphorylation (Violin et al., 2003; Kunkel et al., 2005, 2007; Johnson et al., 2007; Fuller et al., 2008).

The INCENP and Borealin siRNA vectors (gifts from S.M.A Lens, University Medical Center Utrecht, Utrecht, Netherlands) were previously described (Vader et al., 2006). Depletion of INCENP and Borealin was assessed by Western blotting (Fig. S1, A and B) and by immunofluorescence, which showed that the depleted protein was undetectable in ≥90% of mitotic cells. The INCENP rescue constructs are siRNA resistant and are tagged with mCherry as described in this section. We analyzed cells with similar expression levels, determined from mCherry fluorescence.

Drug treatments

Monastrol (used at 100 µM), MG132 (10 µM), and ZM447439 (2 µM except where indicated otherwise) were obtained from Tocris Bioscience, and nocodazole (0.33 µM) was obtained from Sigma-Aldrich. For the ZM washout assay, cells were treated with monastrol (to induce monopolar spindles), MG132 (to prevent mitotic exit), and ZM for 1 h. Then, ZM was washed out, and cells were incubated with monastrol and MG132.

Immunofluorescence

For Borealin and Aurora B staining in Figs. 1 and 3, cells were fixed in cold methanol for 10 min. For Aurora B, INCENP, and phospho-INCENP staining (Figs. S1 and S2), cells were fixed in PBS + 4% formaldehyde at 37°C for 10 min. For phospo-H3 Ser10 staining, cells were fixed for 10 min in 4% formaldehyde in PEM buffer (100 mM Pipes, pH 6.9, 10 mM EGTA, and 1 mM $MgCl_2$) with 0.2% Triton X-100. For phospho-Dsn1 staining, cells were preextracted for 3 min in PEM with 0.4% Triton X-100 and then were fixed for 10 min in 4% formaldehyde in PEM with 0.2% Triton X-100. For analysis of cold-stable microtubules, cells were incubated in L-15 medium (Invitrogen) containing 20 mm Hepes, pH 7.3, on ice for 10 min and then were fixed for 10 min in 4% formaldehyde in PEM with 0.2% Triton X-100. The following primary antibodies were used: 1 µg/ml rabbit anti–human Borealin (a gift from H. Funabiki, The Rockefeller University, New York, NY; Sampath et al., 2004), mouse anti–Aurora B monoclonal (1:1,000; BD), rabbit anti–Aurora B polyclonal (1:1,000; ab70238; Abcam), 1 µg/ml rabbit anti–phospho-Dsn1 Ser100 (a gift from I.M. Cheeseman, Whitehead Institute for Biological Research, Cambridge, MA; Welburn et al., 2010), 0.2 µg/ml mouse anti–phospho-H3 Ser10 (Millipore), rabbit anti-INCENP polyclonal (1:1,000; ab36453; Abcam), and mouse anti-INCENP monoclonal (1:1,000; 39259; Active Motif). The phospho-specific rabbit polyclonal antibody against the INCENP C-terminal TSS motif was generated by Thermo Fisher Scientific against immunizing phosphorylated peptide $_{887}$RYHKRT(pS)(pS)AVWNSPC$_{901}$ and is further characterized in Salimian et al. (2011). The secondary antibodies used were Alexa Fluor 488, 594, or 647 conjugates (Invitrogen) used at a 1:500 dilution.

Immunoblotting

Whole cell lysates were prepared from nocodazole-arrested HeLa cells collected by mitotic shake off. Western blot analysis was performed using the following primary antibodies: rabbit anti-INCENP polyclonal (1:4,000; ab36453; Abcam), rabbit anti-Borealin polyclonal (1:500; a gift from S. Wheatley, University of Nottingham, Nottingham, England, UK; Barrett

et al., 2009), mouse anti–Aurora B monoclonal (1:2,000; BD), and mouse antitubulin monoclonal (1:10,000; Sigma-Aldrich).

Image acquisition and processing

For live imaging, HeLa cells were plated on 22 × 22–mm glass coverslips (no. 1.5; Thermo Fisher Scientific) coated with poly-D-lysine (Sigma-Aldrich). Coverslips were mounted in custom-designed Rose chambers using L-15 medium without phenol red (Invitrogen). Temperature was maintained at ∼35°C using either an air stream incubator (ASI 400; Nevtek) or an environmental chamber (Incubator BL; PeCon GmbH).

Images of centromere- and kinetochore-targeted phosphorylation sensors, phospho-Dsn1, cold-stable microtubules, and the chromatin-targeted phosphorylation sensor for analysis of spatial patterns (Figs. 3–5) were acquired with a spinning disk confocal microscope (DM4000; Leica) with a 100× 1.4 NA objective, an XY Piezo-Z stage (Applied Scientific Instrumentation), a spinning disk (Yokogawa), an electron multiplier charge-coupled device camera (ImageEM; Hamamatsu Photonics), and a laser merge module equipped with 440-, 488-, and 593-nm lasers (LMM5; Spectral Applied Research) controlled by MetaMorph software (Molecular Devices). Maximal intensity projections of confocal stacks are shown in the figures. For live imaging of phosphorylation sensors, CFP or TFP was excited at 440 nm, and CFP/TFP and YFP emissions were acquired simultaneously with a beam splitter (Dual-View; Optical Insights, LLC).

For analysis of the phosphorylation sensors, custom software written in MATLAB (MathWorks) was used as previously described (Fuller et al., 2008). In brief, CFP and YFP emissions were aligned by minimizing the correlation coefficient between the two images. Intensity thresholds were selected manually, and the YFP/CFP emission ratio was calculated after background subtraction within the thresholded area. For display of ratio images, pixels outside the thresholded area were set to 0. For line scan measurements of spatial phosphorylation patterns in HeLa cells, lines of 1 pixel in width were drawn from centromeres, with distance = 0 defined as the center of the spot labeled with CB-mCherry or CB-INCENP–mCherry. For line scan measurements in U2OS-LacO cells, lines of 3 pixels in width were drawn from the LacI-INCENP–mCherry locus, with distance = 0 defined as the center of the mCherry spot. The YFP/CFP emission ratio was calculated along these lines using ImageJ software (National Institutes of Health) and averaged over multiple lines from multiple cells.

For analysis of phospho-Dsn1, CB-mCherry was used to define the centromere regions, and phospho-Dsn1 intensity was measured in these regions, background corrected, and averaged over 11 planes collected with 0.2-µm spacing to represent a single cell. The phospho-Dsn1 was then averaged over multiple cells. For analysis of cold-stable microtubules, kinetochores were examined by visual inspection of confocal image stacks to determine whether a microtubule fiber was attached.

Images of Borealin, Aurora B, phospho-H3, INCENP, phospho-INCENP, and the chromatin-targeted sensor for analyses that did not include spatial patterns were acquired on a microscope (DM6000; Leica) with a 63× 1.4 NA objective and a charge-coupled device camera (ORCA-AG; Hamamatsu Photonics) controlled by MetaMorph software. For live imaging of phosphorylation sensors, CFP was excited with CFP excitation filter, and CFP and YFP emissions were acquired sequentially by switching between CFP and YFP emission filters using a filter wheel (Ludl Electronic Products). The YFP/CFP emission ratio in each image was calculated after background subtraction using ImageJ software. For analysis of phospho-H3, the DNA staining (Hoechst 33342) was used to define the chromosome regions; phospho-H3 intensity was measured in these regions after background subtraction and averaged over multiple cells. For analysis of Aurora B recruitment (Fig. S1, C–E), centromeres were defined by mCherry signal, and INCENP and Aurora B staining intensity was measured in these regions after background subtraction. Each data point represents the mean pixel intensity over the centromeres of a single cell.

To average phosphorylation measurements over multiple experiments and to compare different sensors, normalized phosphorylation was calculated from the emission ratios (Fig. 1, C and D) or from phospho-antibody staining (Fig. 2 C). Data were normalized for each experiment on a scale of 0–1, with the range defined by Borealin-depleted or INCENP-depleted cells (value = 0 on the normalized scale) versus control cells with wt CPC (value = 1). For the example shown in Fig. 1 C, the normalized values were calculated as $(d - b)/(a - b)$ for CB^{DBD}-INCENP or $(c - b)/(a - b)$ for wt-INCENP (a–d refer to the values for different experimental conditions as indicated by the labels to the left of the vertical axis in Fig. 1 C). Normalized values were calculated for each individual experiment and then were averaged over multiple experiments.

Photobleaching of CB^{DBD}-INCENP–GFP or CB^{FL}-INCENP–GFP was performed with a 405-nm laser using a FRAP-3D system (Roper Scientific) with MetaMorph software. Images were acquired before bleaching, immediately after bleaching, and then every 10 s for 2.5 min. At each time point, five images were taken with 0.5-µm spacing using the spinning disk confocal system described in this section. To measure photobleaching and recovery, the bleached centromeres were tracked manually, and total intensity after background subtraction was calculated from the image plane with the brightest signal at each time point. Photobleaching as a result of imaging was estimated as ∼10% over the entire time course, based on analysis of unbleached centromeres. Data were normalized by defining the prebleach intensity as 1 and the postbleach as 0 and then averaging over multiple cells.

Online supplemental material

Fig. S1 shows Western blot analyses of Borealin and INCENP depletion by siRNA and shows that recruitment of Aurora B by INCENP does not depend on the C-terminal TSS motif. Fig. S2 shows that LacI-INCENP is highly concentrated and phosphorylated in U2OS-LacO cells. Fig. S3 shows that phosphorylation of endogenous substrates spreads from centromeres during Aurora B activation. Video 1 shows phosphorylation spreading from centromeres after Aurora B activation. Online supplemental material is available at http://www.jcb.org/cgi/content/full/jcb.201103044/DC1.

We thank H. Funabiki, I.M. Cheeseman, S. Wheatley, S.M.A. Lens, and S.M. Janicki for the gifts of reagents and I.M. Cheeseman, T.M. Kapoor, B.E. Black, and E.L. Grishchuk for critical reading of the manuscript and many helpful discussions.

This work was supported by grants from the National Institutes of Health (GM083988), the Searle Scholars Program, and the Penn Genome Frontiers Institute and a grant from the Pennsylvania Department of Health. The Department of Health specifically disclaims responsibility for any analyses, interpretations, or conclusions.

Author contributions: E. Wang, E.R. Ballister, and M.A. Lampson designed the experiments. E. Wang and E.R. Ballister performed the experiments and analyzed the data. E. Wang generated Figs. 1–3, 4 (A–C), 5, and S3, and E.R. Ballister generated Figs. 4 (D–E), S1, and S2. M.A. Lampson wrote the paper.

Submitted: 7 March 2011
Accepted: 19 July 2011

References

Ahonen, L.J., A.M. Kukkonen, J. Pouwels, M.A. Bolton, C.D. Jingle, P.T. Stukenberg, and M.J. Kallio. 2009. Perturbation of Incenp function impedes anaphase chromatid movements and chromosomal passenger protein flux at centromeres. *Chromosoma*. 118:71–84. doi:10.1007/s00412-008-0178-0

Andrews, P.D., Y. Ovechkina, N. Morrice, M. Wagenbach, K. Duncan, L. Wordeman, and J.R. Swedlow. 2004. Aurora B regulates MCAK at the mitotic centromere. *Dev. Cell*. 6:253–268. doi:10.1016/S1534-5807(04)00025-5

Barrett, R.M., T.P. Osborne, and S.P. Wheatley. 2009. Phosphorylation of survivin at threonine 34 inhibits its mitotic function and enhances its cytoprotective activity. *Cell Cycle*. 8:278–283. doi:10.4161/cc.8.2.7587

Beardmore, V.A., L.J. Ahonen, G.J. Gorbsky, and M.J. Kallio. 2004. Survivin dynamics increases at centromeres during G2/M phase transition and is regulated by microtubule-attachment and Aurora B kinase activity. *J. Cell Sci.* 117:4033–4042. doi:10.1242/jcs.01242

Bishop, J.D., and J.M. Schumacher. 2002. Phosphorylation of the carboxyl terminus of inner centromere protein (INCENP) by the Aurora B Kinase stimulates Aurora B kinase activity. *J. Biol. Chem.* 277:27577–27580. doi:10.1074/jbc.C200307200

Cheeseman, I.M., J.S. Chappie, E.M. Wilson-Kubalek, and A. Desai. 2006. The conserved KMN network constitutes the core microtubule-binding site of the kinetochore. *Cell*. 127:983–997. doi:10.1016/j.cell.2006.09.039

DeLuca, J.G., W.E. Gall, C. Ciferri, D. Cimini, A. Musacchio, and E.D. Salmon. 2006. Kinetochore microtubule dynamics and attachment stability are regulated by Hec1. *Cell*. 127:969–982. doi:10.1016/j.cell.2006.09.047

Fuller, B.G., M.A. Lampson, E.A. Foley, S. Rosasco-Nitcher, K.V. Le, P. Tobelmann, D.L. Brautigan, P.T. Stukenberg, and T.M. Kapoor. 2008. Midzone activation of aurora B in anaphase produces an intracellular phosphorylation gradient. *Nature*. 453:1132–1136. doi:10.1038/nature06923

Gadea, B.B., and J.V. Ruderman. 2006. Aurora B is required for mitotic chromatin-induced phosphorylation of Op18/Stathmin. *Proc. Natl. Acad. Sci. USA*. 103:4493–4498. doi:10.1073/pnas.0600702103

Gassmann, R., A. Carvalho, A.J. Henzing, S. Ruchaud, D.F. Hudson, R. Honda, E.A. Nigg, D.L. Gerloff, and W.C. Earnshaw. 2004. Borealin: a novel chromosomal passenger required for stability of the bipolar mitotic spindle. *J. Cell Biol.* 166:179–191. doi:10.1083/jcb.200404001

Hemmerich, P., S. Weidtkamp-Peters, C. Hoischen, L. Schmiedeberg, I. Erliandri, and S. Diekmann. 2008. Dynamics of inner kinetochore assembly and maintenance in living cells. *J. Cell Biol.* 180:1101–1114. doi:10.1083/jcb.200710052

Hendzel, M.J., Y. Wei, M.A. Mancini, A. Van Hooser, T. Ranalli, B.R. Brinkley, D.P. Bazett-Jones, and C.D. Allis. 1997. Mitosis-specific phosphorylation of histone H3 initiates primarily within pericentromeric heterochromatin during G2 and spreads in an ordered fashion coincident with mitotic chromosome condensation. *Chromosoma*. 106:348–360. doi:10.1007/s004120050256

Honda, R., R. Körner, and E.A. Nigg. 2003. Exploring the functional interactions between Aurora B, INCENP, and survivin in mitosis. *Mol. Biol. Cell*. 14:3325–3341. doi:10.1091/mbc.E02-11-0769

Hsu, J.Y., Z.W. Sun, X. Li, M. Reuben, K. Tatchell, D.K. Bishop, J.M. Grushcow, C.J. Brame, J.A. Caldwell, D.F. Hunt, et al. 2000. Mitotic phosphorylation of histone H3 is governed by Ipl1/aurora kinase and Glc7/PP1 phosphatase in budding yeast and nematodes. *Cell*. 102:279–291. doi:10.1016/S0092-8674(00)00034-9

Janicki, S.M., T. Tsukamoto, S.E. Salghetti, W.P. Tansey, R. Sachidanandam, K.V. Prasanth, T. Ried, Y. Shav-Tal, E. Bertrand, R.H. Singer, and D.L. Spector. 2004. From silencing to gene expression: real-time analysis in single cells. *Cell*. 116:683–698. doi:10.1016/S0092-8674(04)00171-0

Johnson, S.A., Z. You, and T. Hunter. 2007. Monitoring ATM kinase activity in living cells. *DNA Repair (Amst.)*. 6:1277–1284. doi:10.1016/j.dnarep.2007.02.025

Kelly, A.E., S.C. Sampath, T.A. Maniar, E.M. Woo, B.T. Chait, and H. Funabiki. 2007. Chromosomal enrichment and activation of the aurora B pathway are coupled to spatially regulate spindle assembly. *Dev. Cell*. 12:31–43. doi:10.1016/j.devcel.2006.11.001

Kim, Y., A.J. Holland, W. Lan, and D.W. Cleveland. 2010. Aurora kinases and protein phosphatase 1 mediate chromosome congression through regulation of CENP-E. *Cell*. 142:444–455. doi:10.1016/j.cell.2010.06.039

Kitajima, T.S., T. Sakuno, K. Ishiguro, S. Iemura, T. Natsume, S.A. Kawashima, and Y. Watanabe. 2006. Shugoshin collaborates with protein phosphatase 2A to protect cohesin. *Nature*. 441:46–52. doi:10.1038/nature04663

Kunkel, M.T., Q. Ni, R.Y. Tsien, J. Zhang, and A.C. Newton. 2005. Spatio-temporal dynamics of protein kinase B/Akt signaling revealed by a genetically encoded fluorescent reporter. *J. Biol. Chem.* 280:5581–5587. doi:10.1074/jbc.M411534200

Kunkel, M.T., A. Toker, R.Y. Tsien, and A.C. Newton. 2007. Calcium-dependent regulation of protein kinase D revealed by a genetically encoded kinase activity reporter. *J. Biol. Chem.* 282:6733–6742. doi:10.1074/jbc.M608086200

Lampson, M.A., K. Renduchitala, A. Khodjakov, and T.M. Kapoor. 2004. Correcting improper chromosome-spindle attachments during cell division. *Nat. Cell Biol.* 6:232–237. doi:10.1038/ncb1102

Lan, W., X. Zhang, S.L. Kline-Smith, S.E. Rosasco, G.A. Barrett-Wilt, J. Shabanowitz, D.F. Hunt, C.E. Walczak, and P.T. Stukenberg. 2004. Aurora B phosphorylates centromeric MCAK and regulates its localization and microtubule depolymerization activity. *Curr. Biol.* 14:273–286.

Liu, D., G. Vader, M.J. Vromans, M.A. Lampson, and S.M. Lens. 2009. Sensing chromosome bi-orientation by spatial separation of aurora B kinase from kinetochore substrates. *Science (New York, NY)*. 323:1350–1353. doi:10.1126/science.1167000

Liu, D., M. Vleugel, C.B. Backer, T. Hori, T. Fukagawa, I.M. Cheeseman, and M.A. Lampson. 2010. Regulated targeting of protein phosphatase 1 to the outer kinetochore by KNL1 opposes Aurora B kinase. *J. Cell Biol.* 188:809–820. doi:10.1083/jcb.201001006

Maresca, T.J., and E.D. Salmon. 2010. Welcome to a new kind of tension: translating kinetochore mechanics into a wait-anaphase signal. *J. Cell Sci.* 123:825–835. doi:10.1242/jcs.064790

Maresca, T.J., A.C. Groen, J.C. Gatlin, R. Ohi, T.J. Mitchison, and E.D. Salmon. 2009. Spindle assembly in the absence of a RanGTP gradient requires localized CPC activity. *Curr. Biol.* 19:1210–1215. doi:10.1016/j.cub.2009.05.061

Mayer, T.U., T.M. Kapoor, S.J. Haggarty, R.W. King, S.L. Schreiber, and T.J. Mitchison. 1999. Small molecule inhibitor of mitotic spindle bipolarity identified in a phenotype-based screen. *Science (New York, NY)*. 286:971–974. doi:10.1126/science.286.5441.971

Murata-Hori, M., and Y.L. Wang. 2002. Both midzone and astral microtubules are involved in the delivery of cytokinesis signals: insights from the mobility of aurora B. *J. Cell Biol.* 159:45–53. doi:10.1083/jcb.200207014

Ohi, R., T. Sapra, J. Howard, and T.J. Mitchison. 2004. Differentiation of cytoplasmic and meiotic spindle assembly MCAK functions by Aurora B-dependent phosphorylation. *Mol. Biol. Cell*. 15:2895–2906. doi:10.1091/mbc.E04-02-0082

Posch, M., G.A. Khoudoli, S. Swift, E.M. King, J.G. Deluca, and J.R. Swedlow. 2010. Sds22 regulates aurora B activity and microtubule-kinetochore interactions at mitosis. *J. Cell Biol.* 191:61–74. doi:10.1083/jcb.200912046

Riedel, C.G., V.L. Katis, Y. Katou, S. Mori, T. Itoh, W. Helmhart, M. Gálová, M. Petronczki, J. Gregan, B. Cetin, et al. 2006. Protein phosphatase 2A protects centromeric sister chromatid cohesion during meiosis I. *Nature*. 441:53–61. doi:10.1038/nature04664

Salimian, K.J., E.R. Ballister, E.M. Smoak, S. Wood, T. Panchenko, M.A. Lampson, and B.E. Black. 2011. Feedback control in sensing chromosome biorientation by the aurora B kinase. *Curr. Biol.* 21:1158–1165. doi:10.1016/j.cub.2011.06.015

Sampath, S.C., R. Ohi, O. Leismann, A. Salic, A. Pozniakovski, and H. Funabiki. 2004. The chromosomal passenger complex is required for chromatin-induced microtubule stabilization and spindle assembly. *Cell*. 118:187–202. doi:10.1016/j.cell.2004.06.026

Santaguida, S., and A. Musacchio. 2009. The life and miracles of kinetochores. *EMBO J.* 28:2511–2531. doi:10.1038/emboj.2009.173

Sessa, F., M. Mapelli, C. Ciferri, C. Tarricone, L.B. Areces, T.R. Schneider, P.T. Stukenberg, and A. Musacchio. 2005. Mechanism of Aurora B activation by INCENP and inhibition by hesperadin. *Mol. Cell*. 18:379–391. doi:10.1016/j.molcel.2005.03.031

Tang, Z., H. Shu, W. Qi, N.A. Mahmood, M.C. Mumby, and H. Yu. 2006. PP2A is required for centromeric localization of Sgo1 and proper chromosome segregation. *Dev. Cell*. 10:575–585. doi:10.1016/j.devcel.2006.03.010

Trinkle-Mulcahy, L., P.D. Andrews, S. Wickramasinghe, J. Sleeman, A. Prescott, Y.W. Lam, C. Lyon, J.R. Swedlow, and A.I. Lamond. 2003. Time-lapse imaging reveals dynamic relocalization of PP1gamma throughout the mammalian cell cycle. *Mol. Biol. Cell*. 14:107–117. doi:10.1091/mbc.E02-07-0376

Tseng, B.S., L. Tan, T.M. Kapoor, and H. Funabiki. 2010. Dual detection of chromosomes and microtubules by the chromosomal passenger complex drives spindle assembly. *Dev. Cell*. 18:903–912. doi:10.1016/j.devcel.2010.05.018

Vader, G., J.J. Kauw, R.H. Medema, and S.M. Lens. 2006. Survivin mediates targeting of the chromosomal passenger complex to the centromere and midbody. *EMBO Rep.* 7:85–92. doi:10.1038/sj.embor.7400562

Violin, J.D., J. Zhang, R.Y. Tsien, and A.C. Newton. 2003. A genetically encoded fluorescent reporter reveals oscillatory phosphorylation by protein kinase C. *J. Cell Biol.* 161:899–909. doi:10.1083/jcb.200302125

Wang, F., J. Dai, J.R. Daum, E. Niedzialkowska, B. Banerjee, P.T. Stukenberg, G.J. Gorbsky, and J.M. Higgins. 2010. Histone H3 Thr-3 phosphorylation by Haspin positions Aurora B at centromeres in mitosis. *Science*. 330:231–235. doi:10.1126/science.1189435

Welburn, J.P., M. Vleugel, D. Liu, J.R. Yates III, M.A. Lampson, T. Fukagawa, and I.M. Cheeseman. 2010. Aurora B phosphorylates spatially distinct targets to differentially regulate the kinetochore-microtubule interface. *Mol. Cell*. 38:383–392. doi:10.1016/j.molcel.2010.02.034

Xu, Z., H. Ogawa, P. Vagnarelli, J.H. Bergmann, D.F. Hudson, S. Ruchaud, T. Fukagawa, W.C. Earnshaw, and K. Samejima. 2009. INCENP-aurora B interactions modulate kinase activity and chromosome passenger complex localization. *J. Cell Biol.* 187:637–653. doi:10.1083/jcb.200906053

Yamagishi, Y., T. Honda, Y. Tanno, and Y. Watanabe. 2010. Two histone marks establish the inner centromere and chromosome bi-orientation. *Science*. 330:239–243. doi:10.1126/science.1194498